Bioorg. Med. Chem. Lett. 47 (2021) 128226

Contents lists available at ScienceDirect

Bioorganic & Medicinal Chemistry Letters

journal homepage: www.elsevier.com/locate/bmcl

Synthesis of novel 1*H*-Pyrazolo[3,4-*b*]pyridine derivatives as DYRK 1A/1B inhibitors

Areum Park [a,b,1], Jieon Hwang [d,e,1], Joo-Youn Lee [a], Eun Ji Heo [c], Yoon-Ju Na [c,g], Sein Kang [c,g], Kyu-Sung Jeong [b], Ki Young Kim [c,g,*], Sang Joon Shin [e,f,*], Hyuk Lee [a,c,*]

[a] *Infectious Diseases Therapeutic Research Center, Korea Research Institute of Chemical Technology, Daejeon 34114, Republic of Korea*
[b] *Department of Chemistry, Yonsei University, Seoul 03722, Republic of Korea*
[c] *Graduate School of New Drug Discovery and Development, Chungnam National University, Daejeon 34134, Republic of Korea*
[d] *Department of Medicine, Yonsei University College of Medicine, Seoul 03722, Republic of Korea*
[e] *Songdang Institute for Cancer Research, Yonsei University College of Medicine, Seoul 03722, Republic of Korea*
[f] *Division of Medical Oncology, Department of Internal Medicine, Yonsei Cancer Center, Yonsei University College of Medicine, Seoul 03722, Republic of Korea*
[g] *Drug Discovery Platform Technology Research Center, Korea Research Institute of Chemical Technology, Daejeon 34114, Republic of Korea*

ARTICLE INFO

Keywords:
DYRK1A
DYRK1B
Kinase Inhibitors
Pyrazolopyridines
Colon cancer
Organoid

ABSTRACT

As DYRK1A and 1B inhibitors, 1*H*-pyrazolo[3,4-*b*]pyridine derivatives were synthesized. Mostly, 3-aryl-5-arylamino compounds (**6**) and 3,5-diaryl compounds (**8** and **9**) were prepared and especially, 3,5-diaryl compound **8** and **9** showed excellent DYRK1B inhibitory enzymatic activities with IC_{50} Values of 3–287 nM. Among them, 3-(4-hydroxyphenyl), 5-(3,4-dihydroxyphenyl)-1*H*-pyrazolo[3,4-*b*]pyridine (**8h**) exhibited the highest inhibitory enzymatic activity (IC_{50} = 3 nM) and cell proliferation inhibitory activity (IC_{50} = 1.6 μM) towards HCT116 colon cancer cells. Also compound **8h** has excellent inhibitory activities in patient-derived colon cancer organoids model as well as in 3D spheroid assay model of SW480 and SW620. The docking study supported that we confirmed that compound **8h** binds to DYRK1B through various hydrogen bonding interactions and hydrophobic interactions.

DYRK (Dual-specificity tyrosine phosphorylation-regulated kinases) belongs to CMGC group, which includes cyclin-dependent kinases (CDKs), mitogen-activated protein kinases (MAPKs), glycogen synthase kinases (GSKs) and CDC-like kinases (CLKs). DYRK family is constituted with DYRK1A, DYRK1B, DYRK2, DYRK3, and DYRK4.[1,2] DYRK1A is one of the most studied DYRK family and upregulation of DYRK1A[3–6] in brain is related with several neurodegenerative diseases including Down syndrome[7,8] and Alzheimer's disease.[9–11] The relevant diseases with DYRK1A were expanded to diverse cancers[12–14] such as lung cancer, cervical cancer, colorectal cancer, melanoma, and acute myeloid leukemia. Recently, it was reported that DYRK1A is engaged in human pancreatic *β*-cell proliferation,[15–19] which led it a potential therapeutic target for diabetes.[20,21] The DYRK1B is associated with cancer biology and muscle differentiation, and overexpressed in many types of cancer cells such as glioblastoma,[22] breast cancer,[23] pancreatic cancer,[24] and ovarian cancer.[25] Also DYRK1B contributes to progress cell cycle from G0/G1 to S phase, therefore, inhibition of DYRK1B reactivates cancer cells from quiescent state.[26,27] In this reason, the development of DYRK1B inhibitors are mostly concentrated on the treatment of oncolytic diseases (Fig. 1).[28] So far several DYRK1A and 1B inhibitors have entered clinical trials. As DYRK1A inhibitors, Lorecivivint[29] is undergoing phase III trial as a treatment of osteoarthritis and epgigallocatechin-gallate (EGCG) from green tea is in phase II/III clinical trial for cancer immunotherapy. Besides, many DYRK1A and 1B inhibitors are under investigation in the preclinical stage with diverse indications. AZ191[25] has been studied as oncolytic drugs and the GNF-4877[30] is under development as antidiabetic drug. Harmine[31,32] and ProINDY[33] from natural products have been studied for various disease, and based on their structures, azaindole and benzothiazoylidene other novel DYRK1 inhibitors have been designed and synthesized. Leucettamine L41[34] from the marine sponge leucettamine is also under preclinical study for neurodegenerative disease. DANDY[35] is also an azaindole-based compounds, and recently it is reported that one of fluoro-DANDY derivatives has cognitive rescuing effect by *in vivo* study

* Corresponding authors.
E-mail addresses: kykim@krict.re.kr (K.Y. Kim), ssj338@yuhs.ac (S.J. Shin), leeh@krict.re.kr (H. Lee).
[1] These authors contributed equally.

https://doi.org/10.1016/j.bmcl.2021.128226
Received 11 May 2021; Received in revised form 16 June 2021; Accepted 20 June 2021
Available online 26 June 2021
0960-894X/© 2021 Elsevier Ltd. All rights reserved.

of standard mouse model of Down syndrome.[36]

We are interested in 1*H*-pyrazolo[3,4-*b*]pyridine core for developing novel DYRK inhibitors, which has additional nitrogen in azaindole core. We believed this core structure could provide improved activities against DYRK1A/1B and novel characteristics of compound properties. So we prepared diverse 1*H*-pyrazolo[3,4-*b*]pyridine derivatives and examined the cytotoxicity of them against colorectal cancer cell lines.

From the Commercially available 5-bromo-1*H*-pyrazolo[3,4-*b*]pyridine **1**, mono-substituted DYRK 1A/1B inhibitors were firstly synthesized. For the modification on the *C3* position of compound **1**, iodination at the *C3* position of **1** with I_2 was performed. Then the resulting **2** was *N*-protected by a SEM group with trimethylsilylethoxymethyl chloride (SEMCl) and the following regioselective Suzuki-miyaura cross-coupling at *C3* position with arylboronic acids afforded *C3*-substituted compound **3a-o** in 47–76% yields. Deprotection of SEM group from **3** resulted in mono-substituted **4a-o**.

With these compounds in hand, inhibitory enzymatic activities of **4a-o** against DYRK1B were examined (Table 1). Staurosporine was used as a reference compound. Most of phenyl-substituted derivatives (**4a-j**) exhibited moderate to excellent inhibitory activities with IC_{50} values in the range of 54–2040 nM, except for 3-methoxyphenyl (**4b**), 3-nitrophenyl (**4c**), and 4-nitrophenyl (**4i**) substituents which had no inhibitory activity. Especially, 4-methoxyphenyl (**4f**) and 4-hydroxy (**4g**) compounds showed the highest inhibitory activities with IC_{50} values in the range of 54 and 87 nM, respectively. When heteroaromatic substitutes were introduced into 1*H*-pyrazolo[3,4-*b*]pyridine, the IC_{50} values of them (**4k-o**) against DYRK1B were ranged from 121 to 4,038 nM. We selected four compounds (**4e**, **4g**, **4j**, and **4m**) to test DYRK1A inhibitory activities and their IC_{50} values appeared similar compared to those against DYRK1B.

Next, we synthesized di-substituted 1*H*-pyrazolo[3,4-*b*]pyridine derivatives to increase the inhibitory activity against DYRK1B (Scheme 2). Based on compound **3** in Scheme 1, the C—N bond coupling of **3** with arylamines in the presence of Pd_2dba_3 and Xantphos and the following deprotection of SEM group from the corresponding products by TBAF afforded 3-aryl-5-arylamino-1*H*-pyrazolo[3,4-*b*]pyridines (**6a-g**). In another way, consecutive Suzuki-miyaura cross-coupling of **3** with arylboronic acids resulted in *N*-SEM-protected 3,5-diaryl-1*H*-pyrazolo [3,4-*b*]pyridines (**7a-j**) in 61–99% yields. Subsequent deprotection of **7** gave rise to diaryl compounds (**8a-j**). During the process, 4-aminophenyl compound **7k** was followed by the additional reaction with CH_3SO_2Cl,

Table 1

Inhibitory enzymatic activities of compounds **4**.

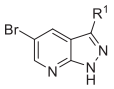

Compound	R^1	DYRK1B IC_{50} (nM)[a,b]
4a		2040
4b		>5 μM
4c		>5 μM
4d		635
4e	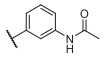	257
4f		54
4g		87
4h	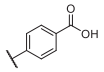	1050
4i		>5 μM
4j	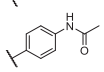	568
4k		615
4l		4038
4m		141
4n		736
4o	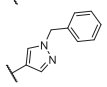	121
Staurosporine		3

[a] IC_{50} values were determined from concentration-dependent inhibition curves of triplicate experiments by GraphPad Prism software.

[b] DYRK1A enzymatic activities (IC_{50}) for the selected compounds : **4e** (638 nM), **4g** (56 nM), **4j** (1,107 nM), and **4m** (92 nM)

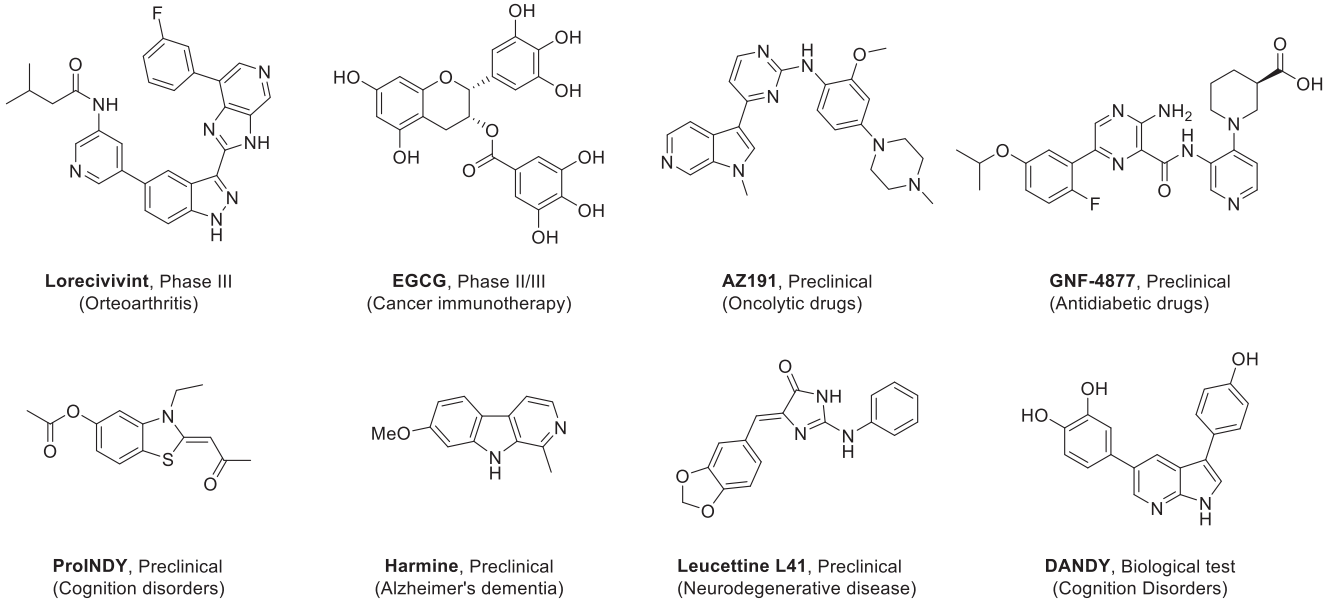

Fig. 1. DYRK inhibitors and their development status.

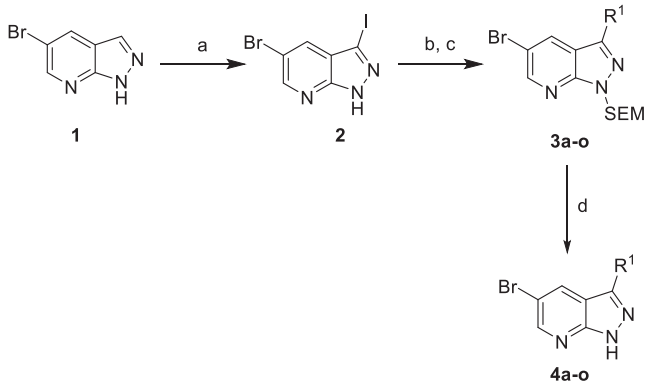

Scheme 1. Reagents and conditions (a) I_2 (1.1 equiv), KOH (2.1 equiv), DMF, rt, 2 h, 83%; (b) SEMCl (1.7 equiv), NaH (2.0 equiv), DMF, rt, 2 h, 95%; (c) R-B$(OH)_2$ (1.1 equiv), Pd(dppf)Cl_2·CH_2Cl_2 (5 mol%), 2 M K_2CO_3 (3.0 equiv), CH_3CN, 85 ℃, 3 h, 47–76%; (d) TBAF (20.0 equiv), THF, reflux, 4 h, 29–99%.

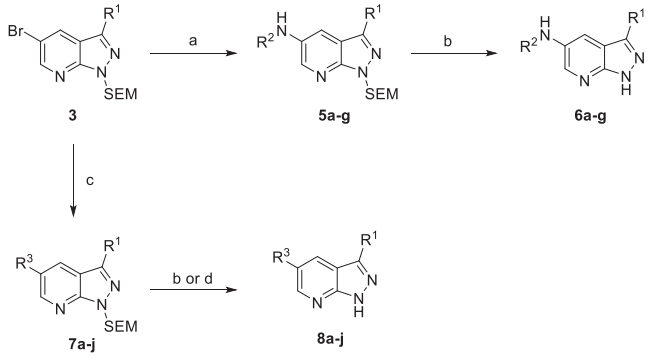

Scheme 2. Reagents and conditions (a) Pd_2dba_3 (10 mol%), Xantphos (10 mol %), Cs_2CO_3 (2.0 equiv), 1,4-dioxane, 90 ℃, 12 h, 44–76%; (b) TBAF (20.0 equiv), THF, reflux, 4 h, 31–62%; (c) R-B$(OH)_2$ (1.1 equiv), Pd(dppf)Cl_2·CH_2Cl_2 (5 mol%), 2 M K_2CO_3 (3.0 equiv), CH_3CN, 85 ℃, 3 h, 61–99%; (d) BBr_3 (10.0 equiv), DCM, rt, 24 h, 24–74%.

Ac_2O, and potassium cyanate (NCOK) to obtain the corresponding products (**9a-e**) (Scheme 3).

When 3-aryl-5-arylamino-1*H*-pyrazolo[3,4-*b*]pyridines (**6a-g**) were tested for the inhibitory activities of DYRK1B, their IC_{50} values slightly improved compared to mono-substituted **4** (Table 2). When compare to **4b** with 4-methoxyphenyl substituent, additional phenylamino (**6a**), 3-hydroxyphenylamino (**6b**), and 3-benzyloxyphenylamino (**6c**) substituents enhanced DYRK 1B inhibitory activities with IC_{50} values of 575 nM, 191 nM, and 3,683 nM, respectively. But, extra arylamino substituents (**6d**, **6f**, and **6g**) into **4f** remained less effective against DYRK1B, and only **6e** showed similar to **4f**. The inhibitory activities of **6a-g** against DYRK1A are also very similar to those against DYRK 1B.

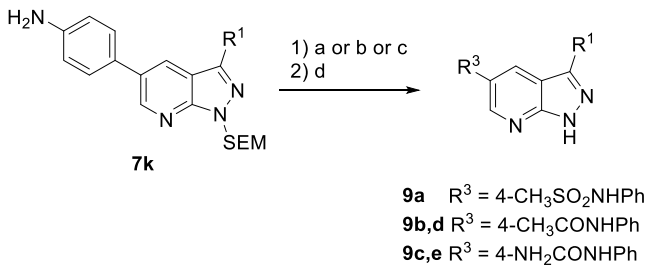

Scheme 3. Reagents and conditions. (a) CH_3SO_2Cl (2.0 equiv), DCM, rt, 12 h, 90%; (b) Ac_2O (1.5 equiv), AcOH, 110 ℃, 5 h, 65%; (c) NCOK (1.2 equiv), 2 N HCl, 0 ℃ to rt, 6 h, 80%; (d) TBAF (20.0 equiv), THF, reflux, 4 h, 37–67%.

Table 2

Inhibitory enzymatic activities of compounds **6**

Compound	R^2	R^1	DYRK 1A IC_{50} (nM)[a]	DYRK 1B IC_{50} (nM)[a]
6a			2817	575
6b	HO		950	191
6c	O		>5 μM	3683
6d			365	188
6e	HO		33	31
6f	O		309	309
6g	F_3C, CF_3		3553	1273
Staurosporine			11	3

[a] IC_{50} values were determined from concentration-dependent inhibition curves of triplicate experiments by GraphPad Prism software.

Most of diaryl 1*H*-pyrazolo[3,4-*b*]pyridine derivatives **8** and **9** showed more improved inhibitory activities against DYRK 1B than compounds **6a-g**, except for **8a** with 3,4-diphenyl substituents (Table 3). With 3,4-dimethoxyphenyl substituent at *C5* position, the derivatization of diverse aryl substituents at *C3* position gave rise to the range of IC_{50} values of 97–287 nM against DYRK 1B (Table 3, 8b-d). When 4-hydroxylphenyl substituent (**8e-f**) was introduced, the inhibitory activities were highly increased from IC_{50} 6 to 56 nM. But, 3-hydroxyphenyl substituent (**8g**) was not effective as much as 4-hydroxyphenyl substituent. Most compounds with 3,4-hydroxyphenyl group **(8h-j)** exhibited the highest inhibitory activities with IC_{50} values of 3–29 nM. Methylsulfonylamino, acylamino and ureido substituents also increased DYRK 1B inhibitory activities with IC_{50} values of 2–13 nM (Table 3, 9a-e). In terms of DYRK 1A, most results of diaryl 1*H*-pyrazolo[3,4-*b*]pyridine derivatives were comparable to those of DYRK 1B.

With the enzymatic activities of DYRK1B inhibitors, the cytotoxic activities against colon cancer cells (HCT116) were investigated. Firstly, several compounds (**8h**, **9a**, **9b**, **9c**, and **9e**) were selected and tested. Among them, compounds **8h**, **9a**, and **9b** showed excellent cell proliferation inhibitory activities with IC_{50} values of 3.4, 1.6, and 2.1 μM, respectively. Rest of compounds **9b** and **9c** remained with IC_{50} values of 16.2 and 8.9 μM, respectively (see supplementary data Fig. S1). After considering their Inhibitory enzymatic, cell proliferation inhibitory activities and other chemical properties including solubilities, we decided to further examine **8h**.

To figure out the effect of **8h** on cytotoxicity towards colon cancer cells, we measured cell proliferation inhibitory activity in 10 colon cancer cell lines (RKO, HCT116, DLD-1, SW620, SW480, COLO205, HT29, LOVO, HCT15, and LS174T). Compound **8h** showed remarkable cytotoxic efficacy against five colon cancer cells such as RKO, HCT116, DLD-1, SW480 and SW620 and exhibited divergent sensitivity (IC_{50} values of 1–38 μM) (Fig. 2a). In addition, the morphology of cells treated with **8h** showed multi-vesicle formation compared to vehicle-treated cells (Fig. 2b). Therefore, we could predict the induction of autophagy by **8h** since they showed the morphologically specific form of autophagic cell death.

Next, we assessed cell growth inhibitory effect through 3D spheroid model that the microenvironment of cancer cell was more resembled that of a patient's tumor tissues (Fig. 3). At day 10 after the treatment of **8h**, the cell size of SW480 and SW620 was reduced. The number of

Table 3
Inhibitory enzymatic activities of diaryl 1*H*-pyrazolo[3,4-*b*]pyridine derivatives.

Compound	R^3	R^1	DYRK 1A IC_{50} (nM)[a,b]	DYRK 1B IC_{50} (nM)[a]
8a			>5 μM	>5 μM
8b			75	97
8c			632	287
8d			299	167
8e			44	56
8f			5	6
8g			213	39
8h			5	3
8i			24	29
8j			NT.	15
9a			NT	5
9b			NT	13
9c			8	7
9d			NT	10
9e			NT	2
Staurosporine			11	3

[a] IC_{50} values were determined from concentration-dependent inhibition curves of triplicate experiments by GraphPad Prism software.
[b] NT: Not tested.

viable cells stained with calcein AM decreased and the size of nuclei stained with Hoechst33342 became smaller. In addition, we found that the number of dead cells stained with ethidium homodimer-1 (EthD-1) increased (Fig. 3). Therefore, the cytotoxic activity of DYRK1 inhibitor **8h** towards SW480 and SW620 colon cancer cells continued to maintain in 3D spheroid models of them.

Finally, we verified the cytotoxic effect of **8h** in patient derived cancer organoid models. As shown in Fig. 4, the treatment of **8h** exhibited reduction of crypt size and disruption of intact organoid structure compared to that of vehicle-treated organoids. Altogether, DYRK1 inhibitor, **8h**, showed prominent cytotoxic effect in colon cancer cell lines through diverse models.

In order to predict the binding modes of compound **8h** for DYRK1B, we performed molecular docking studies with DYRK1B homology model. As shown in Fig. 5, the 1*H*-pyrazolo[3,4-*b*]pyridine scaffold of compound **8h** forms two hydrogen bonds with Glu191 backbone CO and Leu193 backbone NH in the hinge region. Also the 1*H*-pyrazolo[3,4-*b*] pyridine ring forms hydrophobic interactions with Ala138, Val174 and Leu246, as well as 1,2-dihydroxyphenyl ring is oriented towards solvent exposed area by forming hydrophobic interaction with Ile117 and hydrogen bonding with Ile117 backbone CO. Phenol ring makes electrostatic interaction with Lys140, and hydrophobic interaction with Val258.

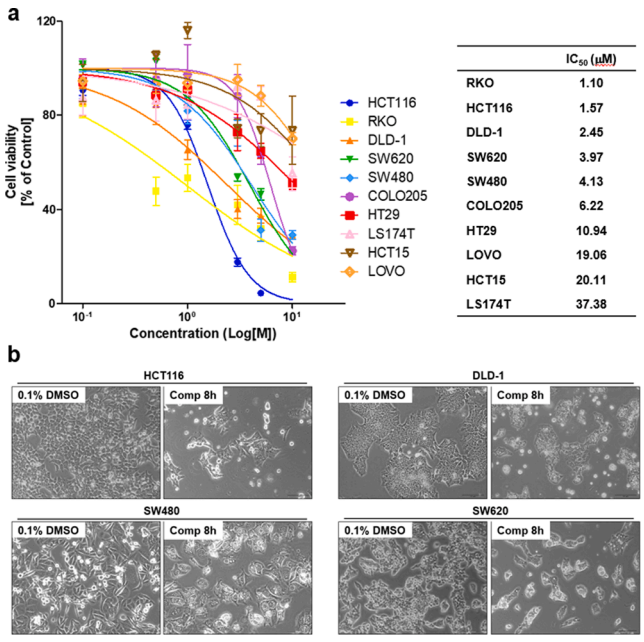

Fig. 2. Cytotoxicity and cells morphology treated with compound **8h**.

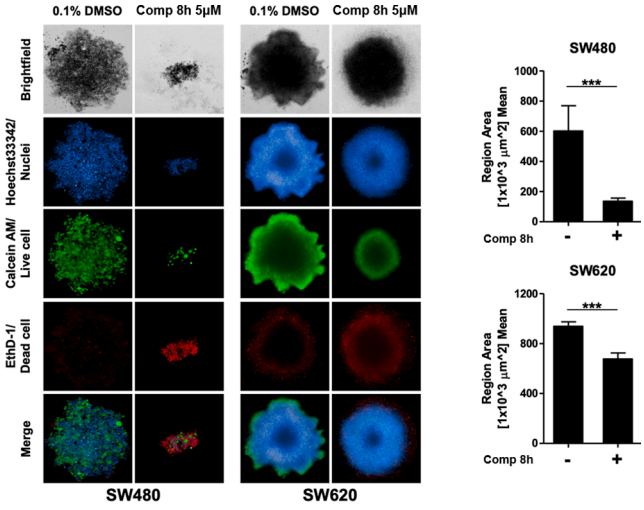

Fig. 3. 3D spheroid assay with compound **8h**. Cells (SW480: 1×10^2 per well and SW620: $1x10^3$ per well) were seeded at 96 well U-bottom plate coated with poly-HEMA. At 3, 5, 7 days, cells were treated with compound **8h** (5 μM). Then, cells were stained with Hoechst33342 (Nuclei), Calcein AM (Live cell) and Ethidium Homodimer-1 (Dead cell). Representative images were taken on day 10 at 50X.

In conclusion, we successfully designed and synthesized 1*H*-pyrazolo [3,4-*b*]pyridine derivatives. Mainly, 3,5-disubstituted 1*H*-pyrazolo[3,4-*b*]pyridines, 3-aryl-5-arylamino compounds (**6**) and 3,5-diaryl compounds (**8** and **9**), were prepared and especially, compound **8** and **9** showed excellent DYRK1B inhibitory enzymatic activities with IC_{50} values of 3–287 nM. Among them, 3-(4-hydroxyphenyl), 5-(3,4-dihydroxyphenyl)-1*H*-pyrazolo[3,4-*b*]pyridine (**8h**) exhibited the highest enzymatic (IC_{50} = 3 nM) and cell proliferation inhibitory activities (HCT116, IC_{50} = 1.6 μM). Also compound **8h** has excellent inhibitory activities in patient-derived colon cancer organoids model as well as in 3D spheroid assay model of SW480 and SW620. The docking study supported that we confirmed that compound **8h** binds to DYRK1B through various hydrogen bonding interactions and hydrophobic interactions.

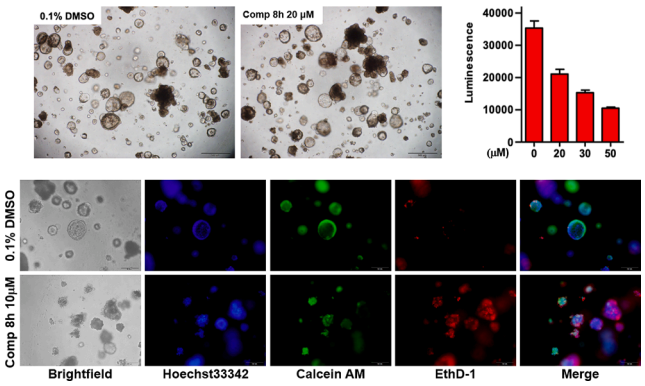

Fig. 4. Cytotoxic effect of compound **8h** in patient-derived organoid model. Colon cancer organoids were treated with **8h** for 5 days and were subjected to cytotoxicity assay using CellTiter Glo. Representative images were taken on day 5 at 50X. Then, organoids were stained with Hoechst33342 (nuclei), Calcein AM (live cell) and Ethidium Homodimer-1 (dead cell). Experiments were performed triplicate and quantified using Prism5.

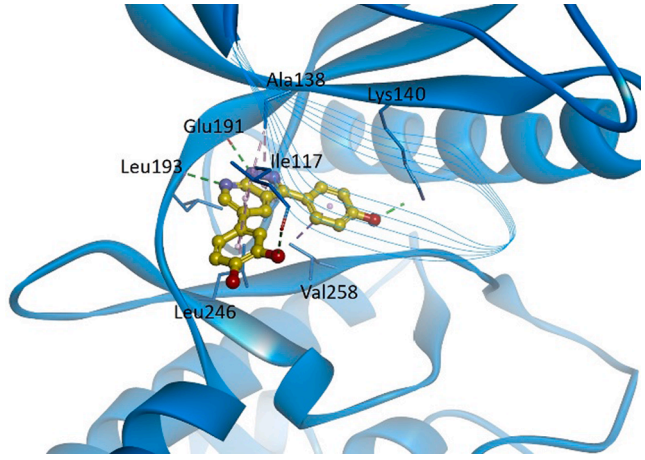

Fig. 5. Docking model of compound **8h** for DYRK1B. Compound **8h** (yellow colored ball and stick) to the DYRK1B (blue colored ribbon). For clarity, key binding site residues are shown in sticks and labeled using the 3-letter amino acid code. The hydrogen bonds are displayed as green dashed lines and hydrophobic interactions are shown as pink dashed lines. Also electrostatic interactions are indicated by orange dashed lines.

Declaration of Competing Interest

The authors declare that they have no known competing financial interests or personal relationships that could have appeared to influence the work reported in this paper.

Acknowledgment

This work was supported by the Korea Research Institute of Chemical Technology [SI-1805-01 (H.L.), KK1803-F00 (K.Y.K) and SI2131-50 (K. Y.K)].

Appendix A. Supplementary data

Supplementary data to this article can be found online at https://doi.org/10.1016/j.bmcl.2021.128226.

References

1 Yoshida K. Role for DYRK family kinases on regulation of apoptosis. *Biochem Pharmacol.* 2008;76:1389–1394.
2 Aranda S, Laguna A, de La Luna S. DYRK family of protein kinases: evolutionary relationships, biochemical properties, and functional roles. *FASEB J.* 2011;25:449–462.
3 Ferrer I, Barrachina M, Puig B, et al. Constitutive Dyrk1A is abnormally expressed in Alzheimer disease, Down syndrome, Pick disease, and related transgenic models. *Neurobiol Dis.* 2005;20:392–400.
4 Ryoo S-R, Jeong HK, Radnaabazar C, et al. DYRK1A-mediated Hyperphosphorylation of Tau. *J Biol Chem.* 2007;282:34850–34857.
5 Wegiel J, Gong C-X, Hwang Y-W. The role of DYRK1A in neurodegenerative disease. *FEBS J.* 2011;278:236–245.
6 Jarhad DB, Mashelkar KM, Kim H-R, Noh M, Jeong LS. Dual-Specificity Tyrosine Phosphorylation-Regulated Kinase 1A (DYRK1A) Inhibitors as Potential Therapeutics. *J Med Chem.* 2018;61:9791–9810.
7 Kim ND, Yoon J, Kim JH, et al. Putative therapeutic agents for the learning and memory deficits of people with Down syndrome. *Bioorg Med Chem Lett.* 2006;16:3772–3776.
8 Liu F, Liang Z, Wegiel J, et al. Overexpression of Dyrk1A contributes to neurofibrillary degeneration in Down syndrome. *FASEB J.* 2008;22:3224–3233.
9 Smith B, Medda F, Gokhale V, Dunckley T, Hulme C. Recent advances in the design, synthesis, and biological evaluation of selective DYRK1A inhibitors: a new for a disease modifying treatment of Alzheimer's disease? *ACS Chem Neurosci.* 2012;3:857–872.
10 Flight MH. Neurodegenerative disease: New kinase targets for Alzheimer's disease. *Nat Rev Drug Discov.* 2013;12:739.
11 Czarna A, Wang J, Zelencova D. Novel Scaffolds for Dual Specificity Tyrosine-Phosphorylation-Regulated Kinase (DYRK1A) Inhibitors. *J Med Chem.* 2018;61:7560–7572.
12 Ionescu A, Dufrasne F, Celbcke M, Jabin I, Kiss R, Lamoral-Theys D. DYRK1A kinase inhibitors with emphasis on cancer. *Mini Rev Med Chem.* 2012;12:1315–1329.
13 Zhou Q, Phoa AF, Abbassi RH, et al. Structural Optimization and Pharmacological Evaluation of Inhibitors Targeting Dual-Specificity Tyrosine Phosphorylation-Regulated Kinases (DYRK) and CDC-like kinase (CLK) in Glioblastoma. *J Med Chem.* 2017;60:2052–2070.
14 Zou T, Yao S, Chen X, et al. LncRNA OIP5-AS1 regulates radioresistance by targeting DYRK1A through miR-369-3p in colorectal cancer cell. *Eur J Cell Biol.* 2018;97:369–378.
15 Rachdi L, Kariyawasam D, Aïello V, et al. Dyrk1A induces pancreatic β cell mass expansion and improves glucose tolerance. *Cell Cycle.* 2014;13(14):2221–2229.
16 Wang P, Alvarez-Perez J-C, Felsenfeld DP, et al. A high-throughput chemical screen reveals that harmine-mediated inhibition of DYRK1A increases human pancreatic beta cell replication. *Nat Med.* 2015;21:383–388.
17 Dirice E, Walpita D, Vetere A, et al. Inhibition of DYRK1A stimulates human β-cell proliferation. *Diabetes.* 2016;65(6):1660–1671.
18 Kumar K, Man-Un Ung P, Wang P, et al. Novel selective thiadiazine DYRK1A inhibitor lead scaffold with human pancreatic β-cell proliferation activity. *Eur J Med Chem.* 2018;157:1005–1016.
19 Ackeifi C, Swartz E, Kumar K, et al. Pharmacologic and genetic approaches define human pancreatic β cell mitogenic targets of DYRK1A inhibitors. *JCI Insight.* 2020;5(1).
20 Huang Z, Tremblay MS, Wu T-H, et al. Discovery of 5-(3,4-difluorophenyl)-3-(pyrazol-4-yl)-7-azaindole (GNF3809) for β-cell survival in type 1 diabetes. *ACS Omega.* 2019;4(2):3571–3581.
21 Liu YA, Jin Q, Zou Y, et al. Selective DYRK1A Inhibitor for the Treatment of Type 1 Diabetes: Discovery of 6-Azaindole Derivative GNF2133. *J Med Chem.* 2020;63:2958–2973.
22 Kettle JG, Ballard P, Bardelle C, et al. Discovery and optimization of a novel series of Dyrk1B kinase inhibitors to explore a MEK resistance hypothesis. *J Med Chem.* 2015;58:2834–2844.
23 Chen Y, Wang S, He A, et al. Dyrk1B overexpression is associated with breast cancer growth and a poor prognosis. *Hum Pathol.* 2017;66:48–58.
24 Friedman E. The Kinase Mirk/dyrk1B: A possible Therapeutic Target in Pancreatic Cancer. *Cancer.* 2010;2(3):1492–1512.
25 Ashford AL, Oxley D, Kettle J, et al. A novel DYRK1B inhibitor AZ191 demonstrates that DYRK1B acts independently of GSK3β to phosphorylate cyclin D1 at Thr^{286}, not Thr^{288}. *Biochem J.* 2014;457:43–56.
26 Friedman E. Mirk/dyrk1B Kinase in Ovarian Cancer. *Int J Mol Sci.* 2013;14:5560–5575.
27 Anderson K, Chen Y, Chen Z, et al. Pyrido[2,3-d]pyrimidines: discovery and preliminary SAR of a novel series of DYRK1B and DYRK1A inhibitors. *Bioorg Med Chem Lett.* 2013;23:6610–6615.
28 Rosenthal AS, Tanega C, Shen M, et al. Potent and selective small molecule inhibitors of specific isoforms of Cdc2-like kinases (Clk) and dual specificity tyrosine phosphorylation-regulated kinase (Dyrk). *Bioorg Med ChemLett.* 2011;21:3152–3158.
29 Deshmukh V, O'Green AL, Bossard C, et al. Modulation of the Wnt pathway through inhibition of CLK2 and DYRK1A by lorecivivint as a novel, potentially disease-modifying approach for knee osteoarthritis treatment. *Osteoarthr Cartil.* 2019;27:1347–1360.
30 Shen W, Taylor B, Jin Q, et al. Inhibition of DYRK1A and GSK3B induces human β-cell proliferation. *Nat Commun.* 2015;6:8381.
31 Göckler N, Jofre G, Papadopoulos C, Soppa U, Tejedor FJ, Becker W. Harmine specifically inhibitors protein kinase DYRK1A and interferes with neurite formation. *FEBS J.* 2009;276:6324–6337.
32 Kumar K, Wang P, Sanchez R, Swartz EA, Stewart AF, DeVita RJ. Development of kinase-selective, harmine-based DYRK1A inhibitors that induce pancreatic human β-cell proliferation. *J Med Chem.* 2018;61:7687–7699.

33 Ogawa Y, Nonaka Y, Goto t. Development of a novel selective Inhibitior of the Down syndrome-related kinase DyrkA. *Nat Commun.* 2010;1:86.
34 Tahtouh T, Elkins JM, Filippakopoulos P, et al. Selectivity, Cocrystal Structures, and Neuroprotective Properties of Leucettines, a Family of Protein Kinase Inhibitors Derived from the Marine Sponge Alkaloid Leucettamine B. *J Med Chem.* 2012;55: 9312–9330.
35 Gourdain S, Dairou J, Denhez C, et al. Development of DANDYs, New 3,5-Diaryl-7-azaindoles Demonstrating Potent DYRK1A Kinase Inhibitory Activity. *J Med Chem.* 2013;56:9569–9585.
36 Neumann F, Gourdain S, Albac C. DYRK1A inhibition and cognitive rescue in a Down syndrome mouse model are induced by new fluoro-DANDY derivatives. *Sci Rep.* 2018;8:2859.